Supplementary Information for: Phase Transformation of Hydrous Ringwoodite to the Lower-Mantle Phases and the Formation of Dense Hydrous Silica

Huawei Chen[1], Kurt Leinenweber[2], Vitali Prakapenka[3], Martin Kunz[4], Hans A. Bechtel[4], Zhenxian Liu[5] and Sang-Heon Shim[1]

[1]School of Earth and Space Exploration, Arizona State University, Tempe, Arizona.

[2]Eyring Materials Center, Arizona State University, Tempe, Arizona.

[3]GeoSoilEnviroCars, University of Chicago, Chicago, Illinois.

[4]Advanced Light Source Division, Lawrence Berkeley National Laboratory, Berkeley, California.

[5]Geophysical Laboratory, Carnegie Institution of Washington, Washington, DC.

Keywords: stishovite, ringwoodite, bridgmanite, periclase, water, mantle

NIR experiments

In the NIR heating, at the position of the main diffraction lines of Rw we observed a broad feature persisting even after 30 min from the appearance of the Stv (or mStv), Brd, and MgO lines. The broader feature of hydrous Rw has much greater width (~3 times greater width) than those of the Stv (or mStv) and Brd lines, indicating that if the Rw phase was not stable at the *P–T* conditions and likely existed in a highly disordered metastable form. CO_2 laser heating provides much larger heating spot and therefore low thermal gradients. Most importantly, hydrous Rw couples directly with a CO_2 laser beam. Because of these reasons, we observed complete transition of Rw to the lower mantle phases. In NIR heating, the heating of the sample relies on coupling of metals (in our case, Pt) and heat conduction to the silicate sample which does not directly couple with the laser. This difference leads to larger thermal gradients in NIR heating even if the thermal insulation layers existed in the sample chamber of DAC.

Although we successfully recovered one sample from the NIR laser heating experiments, because of some amount of metastably persisted hydrous ringwoodite, the H_2O content of the silica may not reflect equilibrium partitioning unlike our CO_2 heating experiments where we found complete conversion of the starting ringwoodite sample to the lower-mantle mineral phases. Thus, we did not include the result from NIR experiments for detailed water content in stishovite.

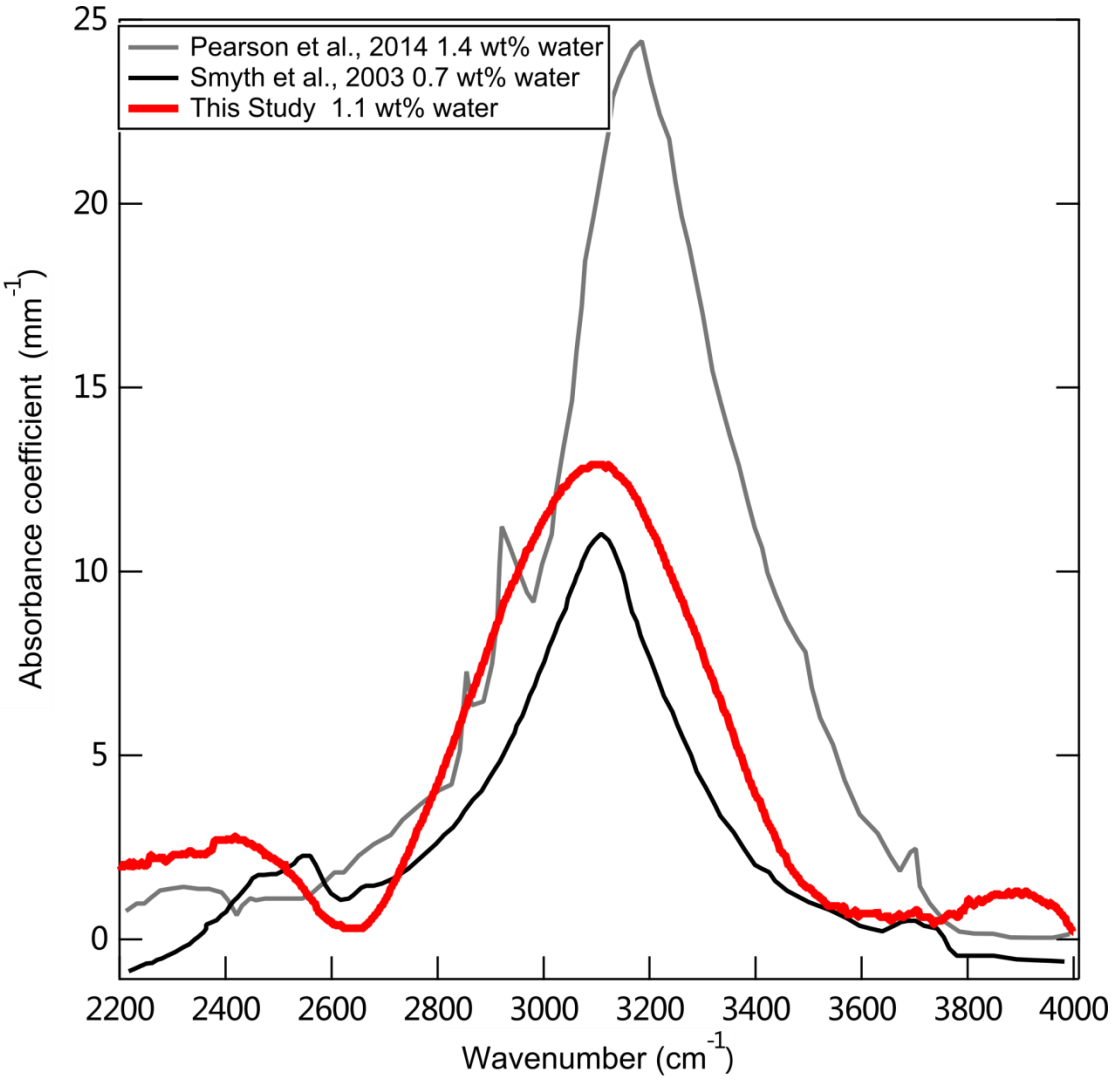

Figure S1, Infrared spectra of hydrous ringwoodite from this study compared with results from Smyth et al. (2003) and Pearson et al. (2014).

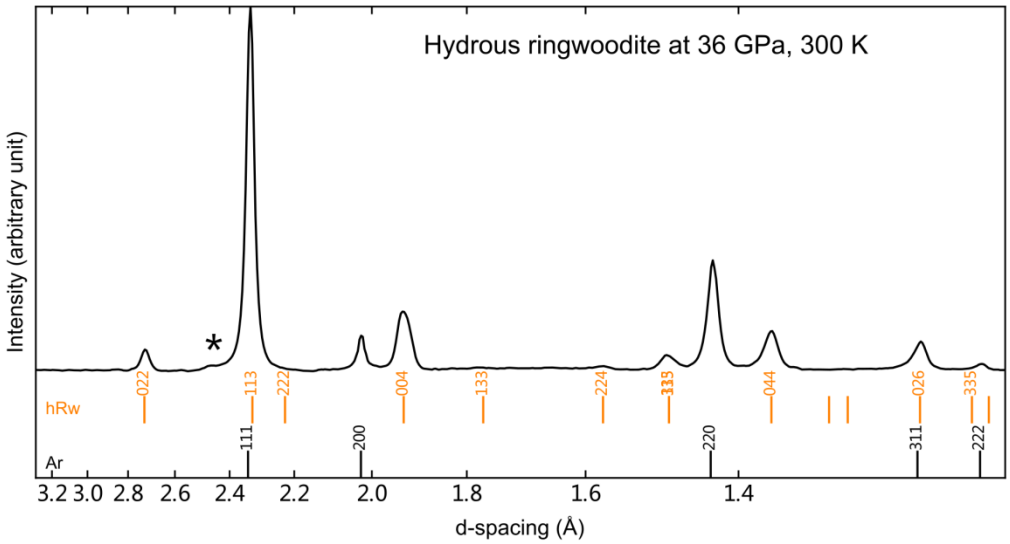

Figure S2, XRD of hydrous ringwoodite from this study at 36 GPa and 300 K. * indicate diffraction line from hcp-Ar.

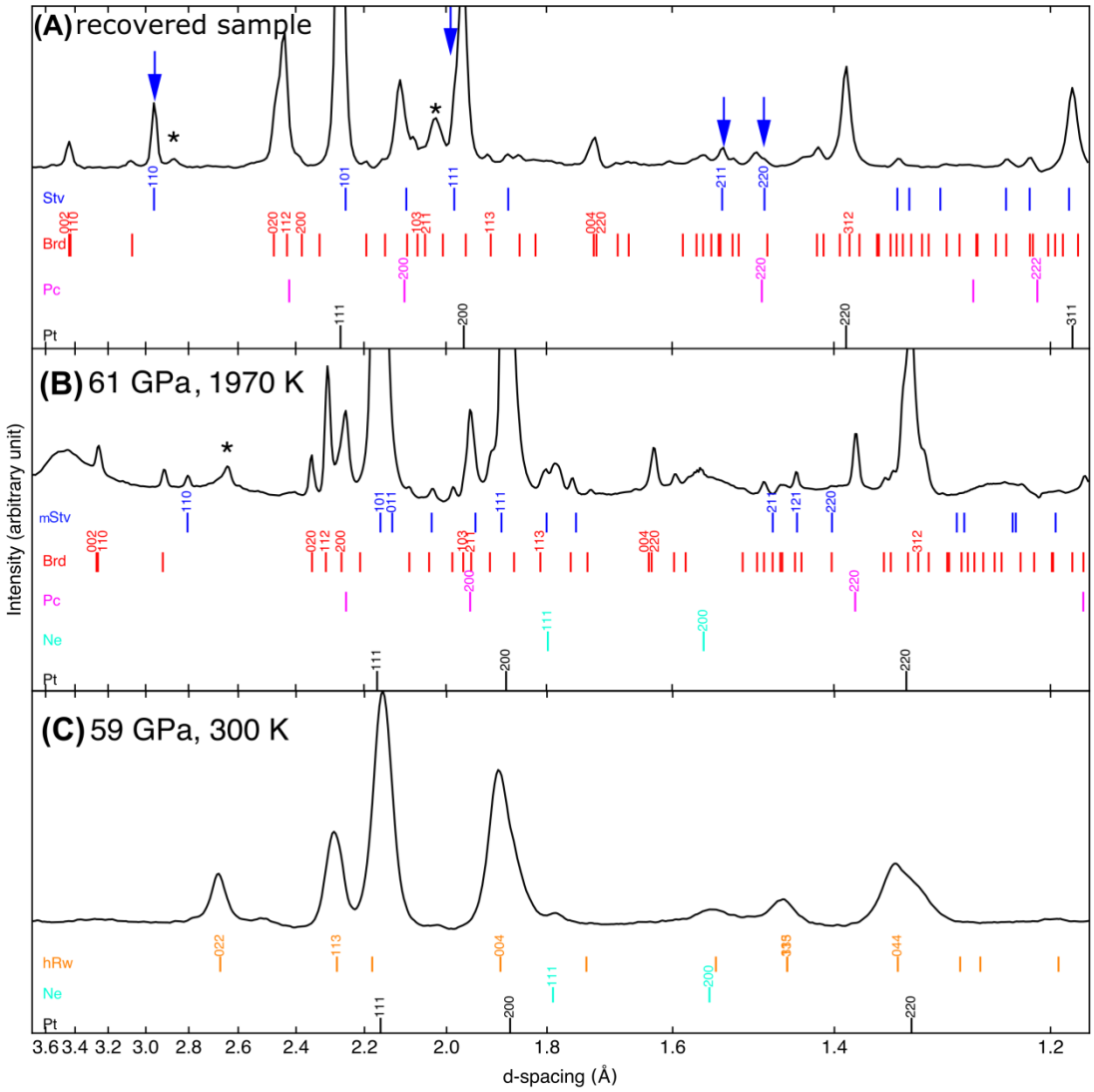

Fig. S3. X-ray diffraction patterns from a NIR laser heating experiment. a, The recovered sample at 1 bar. * indicates the residual ringwoodite peaks. Blue arrows highlight the Stv peaks. b, Formation of lower-mantle mineral phases (Brd, Pc, and Stv) at 61 GPa and 1970 K. c, Hydrous ringwoodite together with a Ne medium and a Pt internal pressure standard (also laser coupler) before heating.

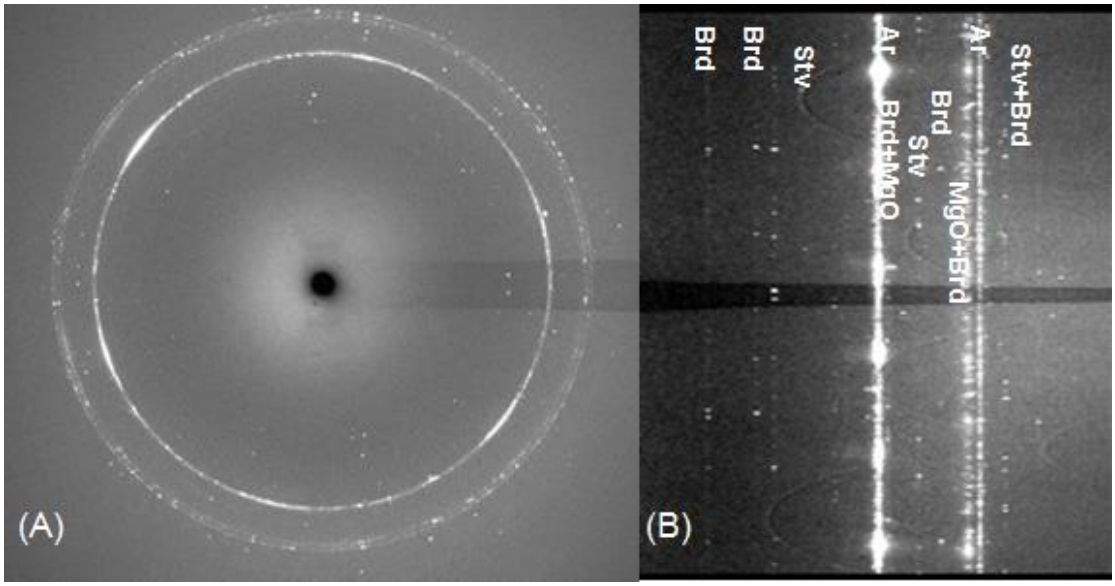

Fig. S4. Two-dimensional X-ray diffraction images (a, raw and b, unrolled) from run203 at 37 GPa and 300 K. We provide labels for all the identified phases.

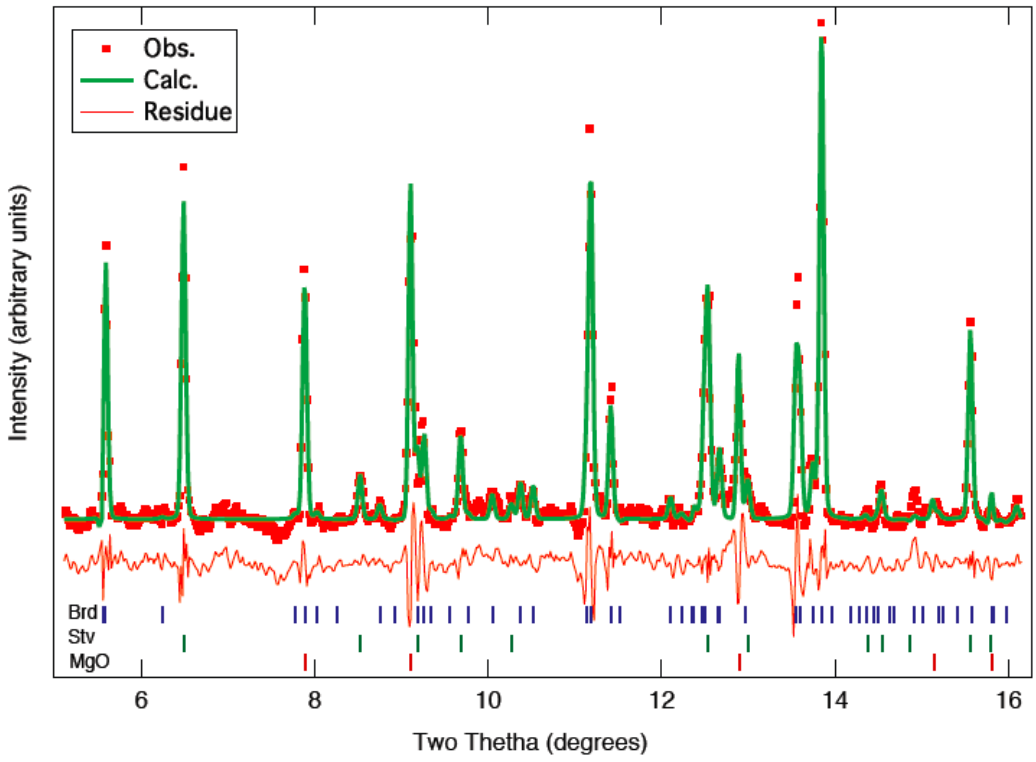

Fig. S5, A Rietveld refinement result for the X-ray diffraction pattern of the sample recovered after synthesis at 50 GPa 1200 K (Tab. 2). The red squares are the measured diffraction intensities. The green curve is the calculated diffraction pattern after fitting in the GSAS-II software. The red line is fit residue after the Rietveld refinement. The ticks at the bottom of the figure show the fitted peak positions for bridgmanite, stishovite, and MgO. The wavelength of the X-ray beam is 0.3344 Å. The fit residue ($R_{wp\text{-}bgnd}$ = 1.8%). The unit-cell volume obtained from the refinements are provided in Tab. 2. We obtain phase fraction of 45 wt% for bridgmanite, 23% for MgO, and 32 wt% for stishovite for this diffraction pattern through Rietveld refinement.